Journal of Fluorescence
https://doi.org/10.1007/s10895-019-02365-5

ORIGINAL ARTICLE

Selective, Sensitive and Label-Free Detection of Fe^{3+} Ion in Tap Water Using Highly Fluorescent Graphene Quantum Dots

Yuanyuan Zhang[1] · Xiangyue Yang[1] · Yunxun Pu[1] · Wei Cheng[1] · Song Lin[1] · Zeyu Shao[1] · Xiaoling Liao[1]

Received: 4 December 2018 / Accepted: 10 March 2019

Abstract
Graphene quantum dots (GQDs) as a new type of fluorescent carbon nanomaterials, showing excellent photoluminescence properties, biocompatibility, photoelectric properties, have become the current research focus. Iron element as an essential element in the human body and an important part of hemoglobin, is very important for human health, so the detection of ferric ions has great significance. In this paper, GQDs with strong blue light emission were prepared through pyrolysis treatment using citric acid as a carbon source. Through characterization by transmission electron microscopy (TEM) and fluorescence spectrometer, it was observed that the GQDs have a uniform particle size distribution and highly fluorescent intensity with a quantum yield of 27.4%. Due to the strong quenching effect of Fe^{3+} on GQDs fluorescence, GQDs was used as a green and facile fluorescence sensor to detect Fe^{3+} selectively and sensitively. The GQDs fluorescence sensor shows a sensitive response to Fe^{3+} in a wide linear range (3.5×10^{-6}-6.7×10^{-4} M), a low detection limit of 1.6 μM ($S/N = 3$) and good selectivity. Importantly, the new sensor realizes the detection of Fe^{3+} ions in tap water because of its low detection limit, wide linear range, and high sensitivity.

Keywords Graphene quantum dots · Fluorescence · Ferric ion · Biosensor · Real sample detection

Introduction

Graphene quantum dots (GQDs) are quasi-zero-dimensional nanomaterials and its internal electrons movement are limited in all directions, so the quantum confinement effect is particularly significant and has many unique properties. This may bring revolutionary changes to the fields of electronics, optoelectronics and electromagnetism. Graphene quantum dots have important potential applications in biology, medicine, materials, new semiconductor devices and other fields [1, 2]. Compared with common semiconductor quantum dots and organic dyes, they have some fascinating advantages, such as excellent biocompatibility, low cytotoxicity, easy preparation, stable photoluminescence property, excellent solubility and tunable adjustable band gaps, therefore making them prospective in biosensing [3–5], bioimaging [6] and metal ion sensing [7–9].

Currently, "top-down" method and "bottom-up" method are developed for the synthesis of GQDs [2, 10]. The former technique involves breaking large size of graphene into small size of graphene quantum dots by using physical or chemical methods like hydrothermal method [11], ionic liquid assisted grinding [12], chemical ablation [13] and electrochemical method [14], etc.; Although these GQDS have desirable quantum yield (QY) values in some cases, the size and thickness of GQDS are generally widely distributed and uneven. However, small carbon molecules can form controllable GQD with adjustable size, shape and performance through a series of bottom-up chemical reactions including solvothermal treatment [15, 16], microwave [17], and thermal pyrolysis [18]. Therefore, the bottom-up approach has obvious advantages, because the composition and properties of GQDs can be easily adjusted by carefully selecting precursors from a variety of organic compounds and controlling carbonization conditions

Yuanyuan Zhang and Xiangyue Yang contributed equally in the article.

✉ Xiaoling Liao
mychtsh@126.com

[1] Chongqing Key Laboratory of Nano/Micro Composite Materials and Devices, Chongqing University of Science and Technology, Chongqing, China

Published online: 22 March 2019

[19]. In addition, improving the QY of GQD is still a great challenge to its application, especially in the field of metal ion sensing [2].

As one of the most important transition metal ions in organisms, Fe^{3+} plays a multifunctional and indispensable role in many physiological processes comprising cell metabolism, oxygen transport and absorption, enzyme catalysis, DNA and RNA synthesis, and electron transfer process [2, 20–22]. The accurate determination of Fe^{3+} concentration becomes an important and effective diagnostic method for monitoring these physiological processes. In addition, the determination of Fe^{3+} concentration in water samples is not only meaningful for human health but also for environmental safety. At present, a variety of analytical techniques for determination of Fe^{3+} concentration have been discovered, including atomic absorption spectrometry [23], spectrophotometry [24], and inductively coupled plasma mass spectrometry [25]. However, these methods require sophisticated instruments and complex sample preparation, which are costly and time-consuming. This has hindered their practical applications in real-time and on-site detection [26]. Fluorescent sensors have become a useful and facile method for the detections of metal ions since they have the advantages of high selectivity, high sensitivity and fast detection [27]. Fluorescent metal nanoparticles and semiconductor quantum dots, as fluorescent sensing materials for metal ion detection, have attracted extensive attention, however, they are limited due to their costly synthesis method and high toxicity. Recently, GQDs as an alternative of semiconductor quantum dots have drawn great attention in metal ion detection because of their relatively low toxicity, good biocompatibility and excellent photostability [28].

In this work, we synthesized graphene quantum dots (GQDs) through a pyrolysis method by using critic acid as a carbon source (Fig. 1). The prepared GQDs have good water-soluble and fluorescence properties. The structures and optical properties of GQDs were detected by fluorescence spectrophotometer, UV spectrophotometer and transmission electron microscope. By using GQDs as a fluorescent probe, the sensitive and selective detection of Fe^{3+} in an aqueous solution was achieved based on the principle that the fluorescence of GQDs can be quenched by Fe^{3+}. Importantly, this method is simple, low cost and has potential application value in actual environmental samples.

Experiment Section

Materials and Instruments

Citric acid was purchased from Chongqing Chemical Reagent Co., Boyi and was used as received. NaOH and absolute ethanol were of analytical grade from Chongqing ChuanDong Chemical Co., Ltd. Rhodamine B is bought from Chengdu Kelong chemical reagent company and was used as received. Water with double distillations was used for the preparation of all the solutions. Chromic acid lotion was used to wash all glassware, and then ethanol and a large amount of ultrapure water were used to rinse all the glassware.

An F97 Pro instrument was used for the fluorescence measurements and the wavelength gap for excitation and emission was set as 5 nm. The UV-vis adsorption spectra were performed on a UV755B UV-visible spectrophotometer. Spectra were usually acquired in a range of 200–700 nm. Transmission Electron Microscopy (TEM) images used for characterizing the size and size distribution of GODs were acquired on a JEM-2100 microscope. A diluted sample solution about 5 μL was spotted on carbon coated copper grid (300 meshes) and then was dried in laboratory atmosphere.

Preparation and Characteristic of GQDs

GQDs were prepared by using citric acid (CA) as a carbon source through a pyrolysis method. Briefly, the preparation method comprises the following steps: (1) putting CA (2.0 g, 10.4 mM) into a beaker, heating the beaker to a temperature of 200 °C through a heating mantle for about 3 min, and stopping heating when the CA became an orange liquid; (2) dissolving the orange liquid in an aqueous solution of NaOH (100.0 mL, 0.25 M), and stirring vigorously for 30 min; and (3) adjusting the pH of the obtained GQDs solution to a range of 6–7 using a NaOH solution, and storing the sample in a 4 °C refrigerator.

Quantum Yield (QY) of GQDs

A comparative method relying on the use of fluorescence standards with known fluorescence quantum yields (Rhodamine B; QY = 95% in our case) is used to calculate the quantum yield. We use the equation:

$$QY_X = QY_S * [A_S/A_X] * [F_X/F_S] * [n_X/n_S]^2$$

where A_x and A_s are the UV absorptions of the sample x and the standard s, respectively; F_x and F_s are the integrated areas under the corrected fluorescence emission spectra of the sample x and the standard s respectively; the n is the refractive indices with $n_x = 1.33$ for water and $n_s = 1.36$ for ethanol. Quantum Yield of Rhodanmine B in ethanol is taken as 0.95.

Briefly, a series of diluted samples GQDs in water and for Rhodamine B at a known concentration (5 μg/mL) were prepared and UV absorption and fluorescence emission scans were performed at the same conditions: same excitation wavelength for the emission scans. Following this, the areas under the curves were determined using Origin software. We use the formula cited above to calculate the quantum yield of GQDs.

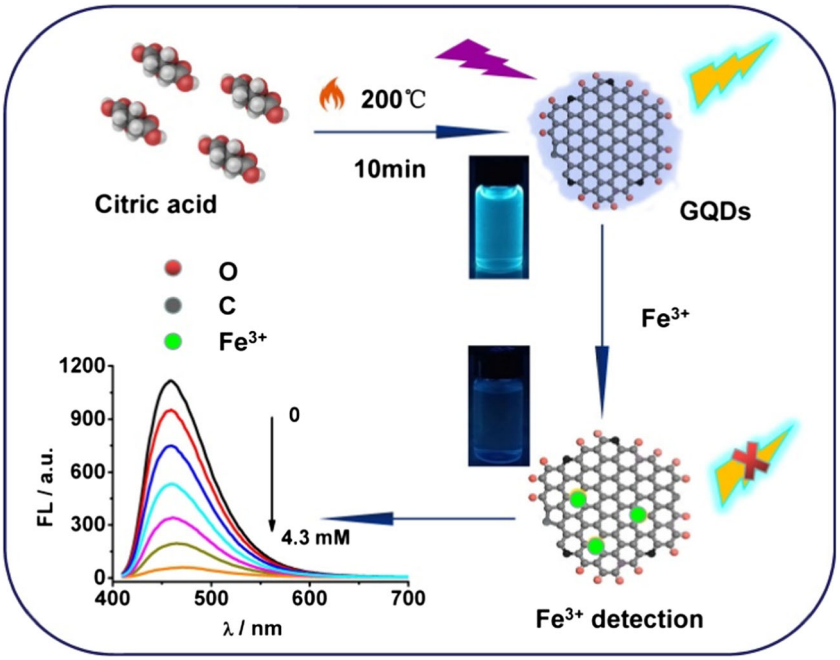

Fig. 1 Schematic of the formation of GQDs and used as a fluorescent probe for Fe^{3+} detection

GQDs for Ion Detection

With GQDs as the detection probe, Fe^{3+} ions were detected in aqueous solution at room temperature. In a typical practice, 150 μL GQDs (40 mg/ml) was added to 10 mL ultra-pure water. Both Fe^{3+} aqueous solutions and other metal ion solutions were freshly prepared before use. In order to investigate the sensitivity of the probe to Fe^{3+}, solutions with different Fe^{3+} concentrations were added into 2 mL GQDs aqueous solution continuously ahead of spectral measurements. The fluorescence spectra were collected at an excitation wavelength of 400 nm on the fluorescence spectrophotometer. Meanwhile, the selectivity of the probe to Fe^{3+} was investigated by detecting the fluorescence response of the probe to other common cations including K^{+}, Mg^{2+}, Na^{+}, Ca^{2+}, Al^{3+}, Cu^{2+}, Sr^{2+}, Cd^{2+}, Co^{2+}, Hg^{2+} and Pb^{2+}.

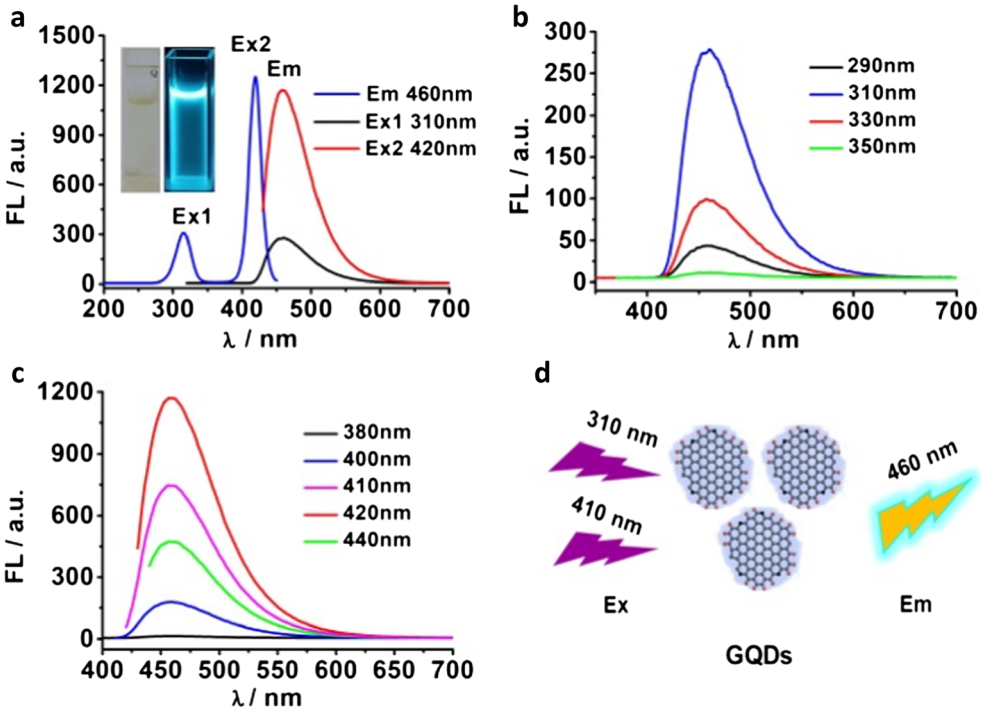

Fig. 2 **a** The excitation spectrum (Ex, blue line) and the emission spectrum (Em, red line) of the GQDs. Inset: Photographs of GQDs in water under visible (left) and UV light (excited at 365 nm; right). **b** Emission spectra of GQDs at 280–330 nm excitation wavelengths. **c** GQDs emission spectra at 400–440 nm excitation wavelengths. **d** The schematic of optical characterization of GQDs with two excitation peaks and one emission peak

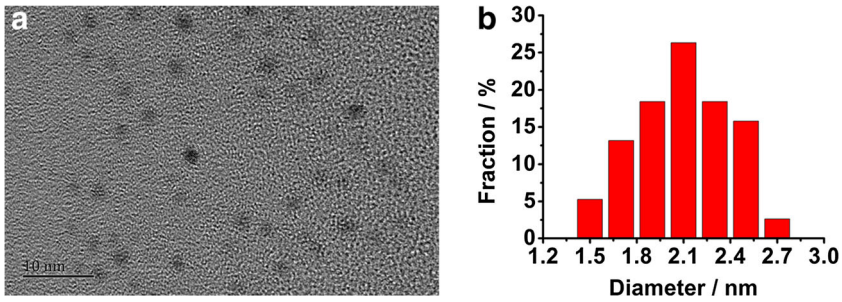

Fig. 3 TEM image (**a**) and diameter distribution (**b**) of the GQDs

Detection of Fe^{3+} in Real Sample

To confirm the practical application of the probe, Fe^{3+} in tap water of our lab were detected after filtering through a 0.22 μm membrane. For the sensitivity measurements, samples with different Fe^{3+} concentrations were prepared to monitor the fluorescence emission spectra.

Result and Discussion

Spectral Characterization of GQDs

Graphene quantum dots (GQDs) were synthesized by utilizing citric acid as a carbon source through a simple and green pyrolysis method. The as-prepared GQDs were clear, and emitted a strong blue fluorescence under a UV lamp (365 nm). As shown in Fig. 2 (A), the as-prepared GQDs was light yellow in an aqueous solution (Fig. 2A, inset left) and emitted an intense blue luminescence under UV lamp (365 nm) (Fig. 2A, inset right). The fluorescence (FL) spectrum shows an emission peak at 460 nm (Fig. 2A, red and black line) and two excitation peaks at 310 nm (Ex1) and 420 nm (Ex2) (Fig. 2A, blue line). Subsequently, 290, 310, 330, and 350 nm, and 380, 400, 410, 420, and 440 nm were selected as excitation wavelengths near the peak of 310 nm and 420 nm respectively, then the emission spectra of GQDs at different excitation wavelengths were obtained (Fig. 2C, D). Although the excitation wavelength changes, the emission wavelength of GQDs remains stable at 460 nm, showing that the GQDs does not have an excitation dependency. The GQDs solution prepared by pyrolysis has high fluorescence intensity and no excitation dependence presenting promising and potential application values as a probe in ion detection.

The size of the as-prepared blue-emitting GQDs is measured by TEM (Fig. 3A). Size analysis shows that the GODs have particles with a diameter of 2.1 nm with a relatively narrow size distribution (Fig. 3B). The quantum yield was calculated to be about 27.4% using the comparative method with Rhodamine B as a standard (QY = 95% in ethanol). This result confirms that the GQDs we prepared have a bright luminescence in water.

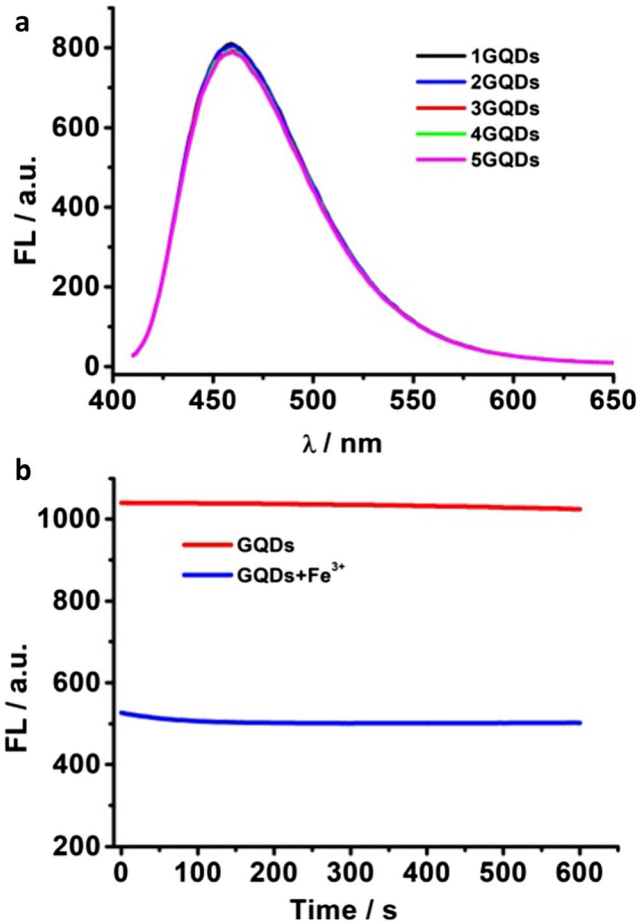

Fig. 4 **a** Fluorescence spectra of GQDs solutions were scanned continuously for five times. **b** Time course curves of GQDs solution in the absence (blue curve) and presence of Fe^{3+} (red curve) in aqueous solution

Sensitive Detection of Fe^{3+} Using GQDs

Iron has empty d orbitals, and the properties of iron ion fluorescence quenching have been reported [29, 30]. Therefore, we supposed that the prepared fluorescent GQDs may be suitable for the effective detection of Fe^{3+}. When the solution with a Fe^{3+} concentration of 1.5 mM was added to GQDs, the fluorescence intensity of GQDs decreased rapidly to half. Importantly, the relevant process of Fe^{3+} quenching GQDs fluorescence was extremely quick and the fluorescence arrived at a steady state within 5 s (Fig. 4B). Surprisingly, the fluorescence intensity of GQDs has no conspicuous decrease within a few days at room temperature, The fluorescence spectrometer scanned GQDs for five consecutive times with almost no decrease (Fig. 4A), indicating that GQDs displayed excellent optical stability and was suitable for the analytical application as a fluorescent probe for quick detection of Fe^{3+} ions.

As shown in Fig. 5, the fluorescence intensity of GQDs probe is sensitive to Fe^{3+} and decreases with the increase of Fe^{3+} concentration. In the absence of Fe^{3+}, GQDs system has a strong fluorescence. When Fe^{3+} was added to GQDs solution, the fluorescence intensity decreased significantly within 5 s. The fluorescence intensity was sensitive to the concentration of Fe^{3+} and decreased in proportion with the increasing of Fe^{3+} concentration (Fig. 5B). In order to demonstrate the sensitivity of this sensing probe, we further investigated the dependence of the quenching effect (F_0/F) on the concentration of Fe^{3+}. The Stern-Volmer equation is suitable for the quenching efficiency [31, 32]:

$$F_0/F = 1 + K_{SV}[Q]$$

Where in F_0 and F are the fluorescence intensities at 460 nm in the absence and presence of Fe^{3+}, respectively. Ksv is the Sterm-Volmer quenching constant, and [Q] is the concentration of Fe^{3+}. Fig. 5C displays a Stern-Volmer curve of GQDs fluorescence quenching by Fe^{3+}, which indicates that there is a good linear correlation with $r^2 = 0.97$ between the fluorescence intensity of GQDs and Fe^{3+} concentration, ranging from 3.5×10^{-6}-6.7×10^{-4} M. The limit of detection (LOD) for Fe^{3+} was 1.6 μM at a signal to noise ratio of 3, which is lower than the maximum level (0.3 mg/L, equivalent to 5.4 μM) of Fe^{3+} allowed in drinking water by the U.S. Environmental Protection Agency. The K_{SV} for Fe^{3+} was measured to be 0.687, which manifested that the GQDs sensing probe had a well affinity to Fe^{3+} ion [33]. Compared to the GQDs or carbon quantum dots (CQDs)-based probes for Fe^{3+} ion detection that have been reported so far (Table 1), although

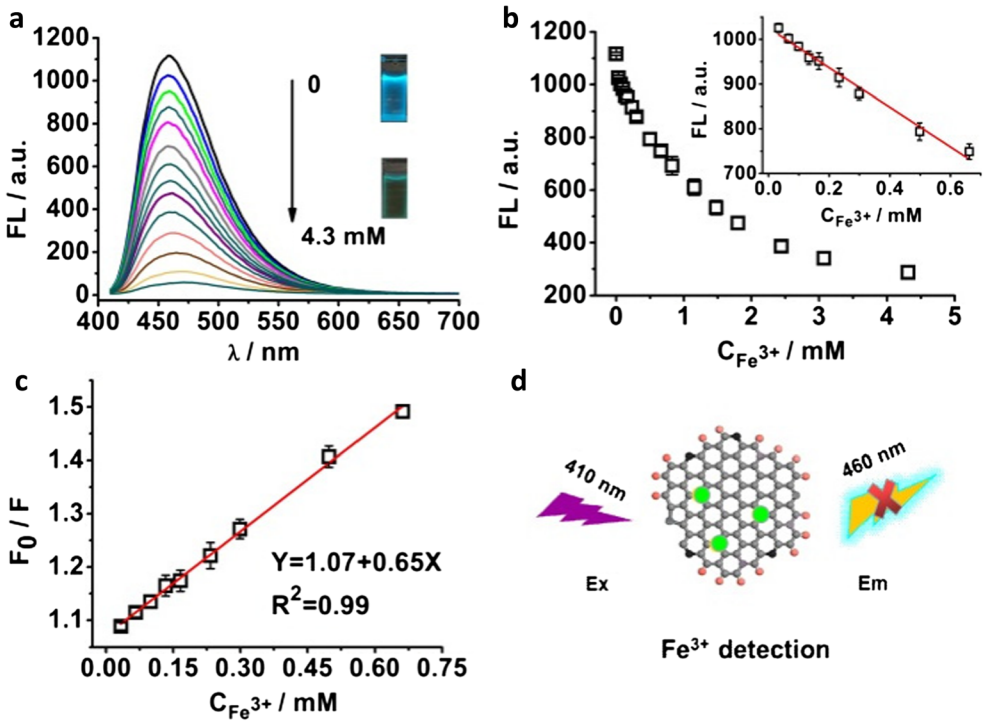

Fig. 5 **a** Fluorescence emission spectra of GQDs (λ_{ex} = 410 nm) in the presence of increasing Fe^{3+} concentrations (1.6×10^{-6}–4.3×10^{-3} M). **b** The relative fluorescence intensity at 460 nm against Fe^{3+} concentration. The error bars represent the standard deviation of three measurements; inset is the linear range of fluorescence quenching of GQDs by Fe^{3+}. **c** The Stern-Volmer plot of fluorescence quenching of GQDs by Fe^{3+}. F_0 and F are the fluorescence intensity of the GQDs at 460 nm in the absence and presence of Fe^{3+}, respectively. **d** The schematic of fluorescence quenching of GQDs by Fe^{3+}

Table 1 Comparison of the detection limit of Fe^{3+} by different sensing probes

Type of probe	Sensing probe	Detection limit (μM)	Reference
GQDs/CQDs-based probe	dopamine functionalized GQDs	0.0076	[2]
	sulfur-doped GQDs	0.0042	[21]
	boron-doped GQDs	0.005	[26]
	sulfur-doped CQDs	0.177	[34]
	Nitrogen and sulfur co-doped CQDs	0.014	[35]
	GQD-BMIM	7.22	[36]
	GQDs	1.6	This work

the detection limit of this work does not reach nanomolar, it can meet specific practical sample application, such as drinking water. In addition, the preparation method of GQDs is simple and green, and the GQDs can be directly used as sensing probe to detect Fe^{3+} ion without further modification such as nitrogen, sulfur or boron doping. The simple preparation method and the good performance of the as-prepared GQDs make the system promising and potential in sensing applications.

To demonstrate the specificity and selectivity of this sensing probe, the fluorescence response of the GQDs to other 12 metal ions at the same concentration was further researched. As indicated in Fig. 6A, the GQDs showed relatively high selectivity for Fe^{3+} over other metal ions. Fig. 6B shows the relative fluorescence intensity of the GQDs in the presence of 1.67 mM Fe^{3+} and other metal ions. We can see that only Fe^{3+} can obviously decrease the fluorescence of the GQDs, and other studied metal ions including K^+, Mg^{2+}, Na^+, Ca^{2+}, Al^{3+}, Cu^{2+}, Zn^{2+}, Sr^{2+}, Cd^{2+}, Co^{2+}, Hg^{2+} and Pb^{2+}, had no significant effect on the fluorescence of GQDs. These results further demonstrated that the GQDs are highly specific to Fe^{3+} over other metal ions, indicating that the good sensitivity and selectivity may allow the sensitive detection of Fe^{3+} in real samples.

To investigate the interaction mechanism of the GQDs to Fe^{3+}, we collected the UV/vis spectra of GQDs solutions before and after addition of Fe^{3+} ions. The spectra were shown in Fig. 7, the ultraviolet absorption curve (blue curve) of a $FeCl_3$ solution shows that the Fe^{3+} ion has an obvious absorption peak at 300 nm. Before the addition of Fe^{3+} ions (black curve), the GQDs solution has an ultraviolet absorption peak at 370 nm. Upon addition of Fe^{3+} ions (red curve), the UV spectrum of GQDs-Fe^{3+} solution did not change at the absorption peak position of 370 nm. Moreover, the UV absorption curves of the solutions before and after adding Fe^{3+} ions were similar (black and red curves). Therefore, it can be inferred that Fe^{3+} ions causing fluorescence quenching of GQDs are at a fluorescence excited singlet state. The excited fluorescent molecule (GQDs) in the excited singlet states collides with the quencher molecule (Fe^{3+}), causing the fluorescence intensity of GQDs by a way of non-radiation transition to the ground state, eventually led to the fluorescence quenching. This is consistent with the literature reports that the adsorption of metal ions onto the graphitic plane of GQDs that is the aggregation-induced fluorescence quenching [33, 34].

Determination of Fe^{3+} in Tap Water Samples

In view of the excellent properties of the above mentioned graphene quantum dot fluorescence sensors, their applications in practical sample analysis were further investigated. As shown in Table 2, tap water was used as a solvent, and solutions with different concentrations of Fe^{3+} ions were dropped into the tap water. A certain amount of the above solutions was

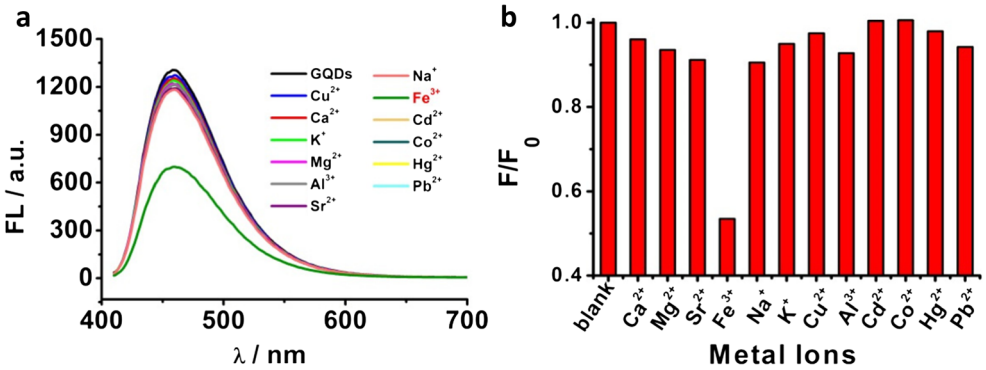

Fig. 6 **a** Fluorescence emission spectra of GQDs with 1.67 mM of 12 different metal ions is added. **b** The fluorescence response histogram of different metal ions to GQDs

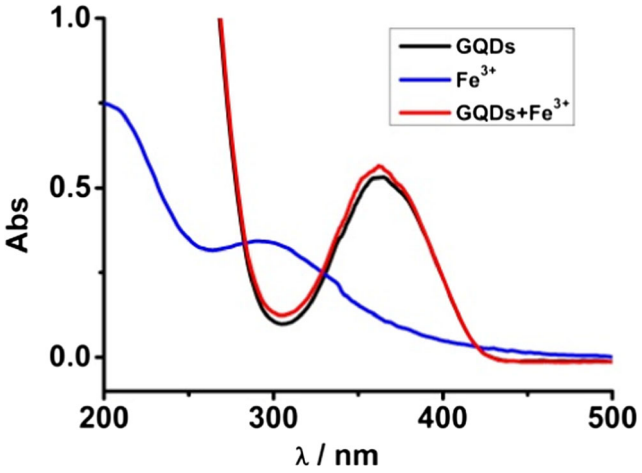

Fig. 7 UV/vis absorption spectrum of Fe^{3+} ionic solution and UV/vis absorption spectra of GQDs solutions before and after the addition of Fe^{3+} ion

added into GQDs solutions to measure the fluorescence intensity at 460 nm. Then, the concentrations of Fe^{3+} are calculated according to the Stern-Volmer curve in Fig. 6. The average relative error between the experimental results and the known concentrations of Fe^{3+} ions in the tap water is below 6%. Therefore, we believed that the prepared fluorescent GQDs could be used as a fluorescent probe to effectively detect Fe^{3+} in tap water.

Conclusions

In this paper, CQDs are prepared through a pyrolysis method which is simple in operation and has an environment-friendly carbon source. The as-prepared GQDs exhibite a blue and stable fluorescence emission at 460 nm with a fluorescence quantum yield about 27.4%. According to the aggregation-induced fluorescence quenching mechanism, the GQDs have high sensitivity, good selectivity, and a detection limit of 1.6 μM for the detection of ferric ion (Fe^{3+}). Furthermore, Fe^{3+} concentrations in real samples (tap water) were analyzed by using this prepared fluorescent sensor, indicating the potential application of GQDs as a fluorescent sensor in biological analysis and environment monitoring.

Acknowledgements This work was supported in part by grants from the National Natural Foundation of China (11532004), Natural Science Key Foundation Project of CQ in China (CSTC2015JCYJBX0003).

Compliance with Ethical Standards

Conflicts of Interest There are no conflicts to declare.

References

1. Shen J, Zhu Y, Yang X, Li C (2012) Graphene quantum dots: emergent nanolights for bioimaging, sensors, catalysis and photovoltaic devices. Cheminform 48(31):3686–3699
2. Dutta CA, Doong RA (2016) Highly sensitive and selective detection of Nanomolar ferric ions using dopamine functionalized graphene quantum dots. ACS Appl Mat Interfaces 8(32):21002–21010
3. Xing L, Shoujun Z, Bin X, Ke M, Junhu Z, Bai Y, Wenjing T (2013) Self-assembled graphene quantum dots induced by cytochrome c: a novel biosensor for trypsin with remarkable fluorescence enhancement. Nanoscale 5(17):7776–7779
4. Liu J, Liu Z, Barrow CJ, Yang W (2015) Molecularly engineered graphene surfaces for sensing applications: a review. Anal Chim Acta 859:1–19
5. Peng J, Gao W, Gupta BK, Liu Z, Romero-Aburto R, Ge L, Song L, Alemany LB, Zhan X, Gao G (2012) Graphene quantum dots derived from carbon fibers. Nano Lett 12(2):844–849
6. Zhu S, Zhang J, Tang S, Qiao C, Wang L, Wang H, Liu X, Li B, Li Y, Yu W (2012) Surface chemistry routes to modulate the photoluminescence of graphene quantum dots: from fluorescence mechanism to up-conversion bioimaging applications. Adv Funct Mater 22(22):4732–4740
7. Tabaraki R, Nateghi A (2016) Nitrogen- doped graphene quantum dots: "turn-off" fluorescent probe for detection of ag(+) ions. J Fluoresc 26(1):297–305
8. Salehnia F, Faridbod F, Dezfuli AS, Ganjali MR, Norouzi P (2016) Cerium(III) ion sensing based on graphene quantum dots fluorescent turn-off. J Fluoresc 27(1):1–8
9. Jiang Y, Wang Z, Dai Z (2016) Preparation of silicon-carbon-based dots@dopamine and its application in intracellular ag(+) detection and cell imaging. ACS Appl Mat Interfaces 8(6):3644–3650
10. Xin Y, Xiao C, Liang-Shi L (2010) Synthesis of large, stable colloidal graphene quantum dots with tunable size. J Am Chem Soc 132(17):5944–5945
11. Sung K, Sung Won H, Min-Kook K, Yeol SD, Hee SD, Oh KC, Seung Bum Y, Jae Hee P, Euyheon H, Suk-Ho C (2012) Anomalous behaviors of visible luminescence from graphene quantum dots: interplay between size and shape. ACS Nano 6(9):8203–8208

Table 2 Experimental results of using GQDs as a fluorescent sensor to detect iron ions in tap water

Tap water sample[a]	Original Fe^{3+} concentration	Standard Fe^{3+} concentration (μM)	Fe^{3+} concentration detected (μM)	Relative error (%)
1	ND[c]	60	57	5
2	ND[c]	200	189	5.5
3	ND[c]	500	511	2.2

[a] Samples 1, 2, and 3 are tap water with 60 μM, 200 μM and 500 μM Fe^{3+} ions, respectively

[b] The experimental results are the mean of three parallel tests

12. Nai Gui S, Pagona P, Surbhi S, Gennady L, Meixian L, Mcneill DW, Quinn AJ, Wuzong Z, Ross B (2012) Controllable selective exfoliation of high-quality graphene nanosheets and nanodots by ionic liquid assisted grinding. Chem Commun 48(13):1877–1879
13. Dengyu P, Jingchun Z, Zhen L, Minghong W (2010) Hydrothermal route for cutting graphene sheets into blue-luminescent graphene quantum dots. Adv Mater 22(6):734–738
14. Yan L, Yue H, Yang Z, Gaoquan S, Lier D, Yanbing H, Liangti Q (2011) An electrochemical avenue to green-luminescent graphene quantum dots as potential electron-acceptors for photovoltaics. Adv Mater 23(6):776–780
15. Deng D, Pan X, Yu L, Cui Y, Jiang Y, Qi J, Li WX, Fu Q, Ma X, Xue Q (2011) Toward N-doped graphene via Solvothermal synthesis. Chem Mater 23(5):1188–1193
16. Feng Y, Zhao J, Yan X, Tang F, Xue Q (2014) Enhancement in the fluorescence of graphene quantum dots by hydrazine hydrate reduction. Carbon 66(3):334–339
17. Li LL, Ji J, Fei R, Wang CZ, Lu Q, Zhang JR, Jiang LP, Zhu JJ (2012) A facile microwave avenue to Electrochemiluminescent two-color graphene quantum dots. Adv Funct Mater 22(14): 2971–2979
18. Ruili L, Dongqing W, Xinliang F, Klaus M (2011) Bottom-up fabrication of photoluminescent graphene quantum dots with uniform morphology. J Am Chem Soc 133(39):15221–15223
19. Dong Y, Shao J, Chen C, Li H, Wang R, Chi Y, Lin X, Chen G (2012) Blue luminescent graphene quantum dots and graphene oxide prepared by tuning the carbonization degree of citric acid. Carbon 50(12):4738–4743
20. Zheng M, Tan H, Xie Z, Zhang L, Jing X, Sun Z (2013) Fast response and high sensitivity europium metal organic framework fluorescent probe with chelating terpyridine sites for Fe(3+). ACS App Mat Interfaces 5(3):1078–1083
21. Li S, Li Y, Cao J, Zhu J, Fan L, Li X (2014) Sulfur-doped graphene quantum dots as a novel fluorescent probe for highly selective and sensitive detection of Fe(3+). Anal Chem 86(20):10201–10207
22. Zecca L, Youdim M, P, Connor J, Crichton R (2004) Iron, brain ageing and neurodegenerative disorders. Nat Rev Neurosci 5 (11): 863–873
23. Sadeghi S, Ashoori V (2016) Sequential determination of iron species in food samples by new task specific ionic liquid based in situ dispersive liquid–liquid microextraction prior to flame atomic absorption spectrometry. Anal Methods 8(25):5031–5038
24. Ju J, Chen W (2014) Synthesis of highly fluorescent nitrogen-doped graphene quantum dots for sensitive, label-free detection of Fe (III) in aqueous media. Biosens Bioelectron 58(10):219–225
25. García-Fernández J, Bettmer J, Jakubowski N, Panne U, Añón E, Montes-Bayón M, Sanz-Medel A (2017) The fate of iron nanoparticles used for treatment of iron deficiency in blood using mass-spectrometry based strategies. Microchim Acta 184(10):3673–3680
26. Li C, Wu C, Pan D, Feng X, Ping W, Cai C (2017) Electrolyzing synthesis of boron-doped graphene quantum dots for fluorescence determination of Fe(3+) ions in water samples. Talanta 164:100–109
27. Zhang Y, Jiang H, Wang X (2015) Cytidine-stabilized gold nanocluster as a fluorescence turn-on and turn-off probe for dual functional detection of ag(+) and hg(2+). Anal Chim Acta 870:1–7
28. Tam TV, Trung NB, Kim HR, Jin SC, Choi WM (2014) One-pot synthesis of N-doped graphene quantum dots as a fluorescent sensing platform for Fe(3+) ions detection. Sensor Actuat B Chem 202: 568–573
29. Lohani CR, Lee K-H (2010) The effect of absorbance of Fe(3+) on the detection of Fe(3+) by fluorescent chemical sensors. Sensor Actuat B Chem 143(2):649–654
30. Liu X, Theil EC (2005) Ferritins: dynamic management of biological iron and oxygen chemistry. Acc Chem Res 38(3):167–175
31. Mu X, Li Q, Ping D, Qiao J, Jian H, Nie Z, Ma H (2013) Facile one-pot synthesis of l -proline-stabilized fluorescent gold nanoclusters and its application as sensing probes for serum iron. Biosens Bioelectron 49(22):249–255
32. J-a AH, Chang H-C, Su W-T (2012) DOPA-mediated reduction allows the facile synthesis of fluorescent gold nanoclusters for use as sensing probes for ferric ions. Anal Chem 84(7):3246–3253
33. Wu Z, Li W, Chen J, Yu C (2014) A graphene quantum dot-based method for the highly sensitive and selective fluorescence turn on detection of biothiols. Talanta 119(4):538–543
34. Ananthanarayanan A, Wang X, Routh P, Sana B, Lim S, Kim DH, Lim KH, Li J, Peng C (2014) Facile synthesis of graphene quantum dots from 3D graphene and their application for Fe(3+) sensing. Adv Funct Mater 24(20):3021–3026
35. Wu F, Yang M, Zhang , Zhu S, Zhu X, Wang K (2018) Facile synthesis of sulfur-doped carbon quantum dots from vitamin b1 for highly selective detection of Fe(3+) ion. Opt Mater 77:258–263
36. Wu H, Jiang J, Gu X, Tong C (2017) Nitrogen and sulfur co-doped carbon quantum dots for highly selective and sensitive fluorescent detection of Fe(3+) ions and l-cysteine. Microchim Acta 184(7): 2291–2298